Spiking synchronization of ion channel clusters on an axon

Shangyou Zeng
Department of Physics, Xiangtan University, Hunan Province 411105 China

Yi Tang
Department of Physics, Xiangtan University, Hunan Province 411105 China

Peter Jung
Department of Physics and Astronomy, Ohio University, Athens, Ohio 45701, USA
(Received 10 January 2007; revised manuscript received 6 May 2007; published 11 July 2007)

Ion channels are distributed in clusters in squid giant axons, rat retinal nerve fiber layers, pyramidal cell dendrites of Apteronotus, etc. Ion channel clusters along the unmyelinated axon generate spontaneous spiking due to ion channel noise. Ion channel clusters are coupled by the axonal cable, and spontaneous spiking of each ion channel cluster can be synchronized. This paper considers the spiking synchronization of two ion channel clusters coupled by an axon. It is shown that axonal parameters affect the spiking synchronization exponentially and ion channel clusters have maximal spiking synchronization when they have the same size. It is further shown that there is an optimal length of the ion channel clusters with maximal spiking synchronization and the optimal length accords with the length of the node of Ranvier in the myelinated axon.

DOI: 10.1103/PhysRevE.76.011905 PACS number(s): 87.19.La, 87.16.Uv

I. INRTODUCTION

Synchronization is a basic phenomenon in science and has many applications in living systems [1]. Periodic self-sustained oscillators adjust oscillating frequencies through synchronization due to weak interactions [2,3]. During the past decade, synchronization has been used to describe the interaction of chaotic oscillators. Recently, the effect of the phase synchronization of chaotic systems has been described [4]. In phase synchronization, phase locking is important, while the amplitude of oscillation is neglected. In living systems, the notion of synchronization is used widely to describe interactions between different physiological systems demonstrating oscillating behavior. There are many synchronization phenomena in living systems, such as phase locking of respiration with locomotory rhythms [5], coordinated movement [6], synchronization of oscillations of human insulin secretion [7], and synchronization of noisy electrosensitive cells in the paddlefish [8].

In neurons, the spiking frequency and time of action potentials can be synchronized by weak interactions. The generation of action potentials is due to the movement of ions across the membrane through ion channels. Ion channels are usually distributed uniformly along the unmyelinated axon to support action potential propagation, but in some cases, ion channels are also distributed in clusters in squid giant axons [9,10], rat retinal nerve fiber layers [11], pyramidal cell dendrites of Apteronotus [12], etc. The ion channel clusters along the unmyelinated axon generate spontaneous spiking due to ion channel noise [13,14], and they can be considered self-sustained oscillators. The ion channel clusters are coupled by an axonal cable, and the spontaneous spiking of each ion channel cluster can be synchronized. This paper considers the spiking synchronization of two ion channel clusters coupled by an axon. First, we calculate the effect of axonal parameters on the spiking synchronization of ion channel clusters along the axon. Then we consider the effect of ion channel cluster size on the spiking synchronization. It is shown that axonal parameters affect the spiking synchronization exponentially and ion channel clusters have maximal spiking synchronization when they have the same size. It is further shown that there is an optimal length of ion channel clusters for which the effect of spiking synchronization is maximal, and the optimal length accords with the length of the node of Ranvier in the myelinated axon.

II. METHODS

A. Deterministic Hodgkin-Huxley equations

The electrical behavior of excitable nerve membranes was first quantitatively formalized by Hodgkin and Huxley (HH) [15]. In HH equations, the voltage depending on ion channel conductance is described by a set of deterministic nonlinear differential equations. When the number of ion channels is large, HH equations are a good approximation to describe the average behavior of numerous ion channels, which individually open and close stochastically. In HH equations, the electrical potential of a neuron cell membrane is formalized by

$$C_m \frac{dV}{dt} = -g_L(V - V_L) - g_K(V - V_K) - g_{Na}(V - V_{Na}) + I, \tag{1}$$

where C_m is the specific capacitance of the membrane, V is the membrane potential, V_L is the reversal potential for the leakage current, V_K is the reversal potential for the potassium ion channel current, V_{Na} is the reversal potential for the sodium ion channel current, g_L is the leakage current conductance, g_K is the potassium ion channel conductance, g_{Na} is the sodium ion channel conductance, and I is the injection current. For a specific membrane, C_m, g_L, V_L, V_K, and V_{Na} are constant; however, g_K and g_{Na} are voltage-dependent variables, which are described by a set of first-order differential equations.

Conductances for potassium and sodium ion channels are

$$g_{\mathrm{K}}(V,t) = \bar{g}_{\mathrm{K}} n^4,$$

$$g_{\mathrm{Na}}(V,t) = \bar{g}_{\mathrm{Na}} m^3 h,$$

where $\bar{g}_{\mathrm{K}}$ and $\bar{g}_{\mathrm{Na}}$ are the maximal conductances of potassium ion channels and sodium ion channels, respectively. The dynamics of gate n (similar for m and h) is given by

$$\frac{dn}{dt} = \alpha_n(1-n) - \beta_n n, \tag{2}$$

where α_n is the transition rate from close state to open state and β_n is the transition rate from open state to close state.

B. Stochastic HH equations

When the ion channel number is small, because the effect of ion channel fluctuations is dramatic, deterministic HH equations are not a good approximation for the average behavior of ion channels. Then stochastic HH equations are more valid to describe the electrical behavior of the membrane. There are four identical n gates in one potassium ion channel, three identical m gates and one h gate in one sodium ion channel. Only when all four identical n gates of one potassium ion channel are in the open state, the potassium ion channel is conducting. Similarly, only when all three identical m gates and the h gate of one sodium ion channel are in the open state is the sodium ion channel conducting. Potassium and sodium ion channel conductances are given by

$$g_{\mathrm{K}}(V,t) = \gamma_{\mathrm{K}}[n_4], \tag{3}$$

$$g_{\mathrm{Na}}(V,t) = \gamma_{\mathrm{Na}}[m_3 h_1], \tag{4}$$

where $[n_4]$ is the number of open potassium ion channels in the unit-area membrane, $[m_3 h_1]$ is the number of open sodium ion channels in the unit-area membrane, γ_{K} is the conductance of each potassium ion channel, and γ_{Na} is the conductance of each sodium ion channel.

Affected by an array of forces, such as random thermal forces, atomic bonds, and electrostatic forces, some ion channels exhibit significant memory effects and non-Markovian characteristics [16–19]. In classical models of voltage-gated ion channels, it is assumed that the switching rates of the ion channel depend only on the present state of the channel [15,20,21]. In this Markov process formulation, the physical state of the ion channel at one time does not depend on its physical state at an earlier time. Incorporating the stochastic behavior of ion channels, a Markov model can be used to formalize the corresponding kinetic model [22]. In the model, one potassium ion channel can exist in five different states and the kinetic scheme is given by Fig. 1 where $[n_i]$ is the number of potassium ion channels with i open gates. So $[n_4]$ is the number of open potassium ion channels (see Fig. 1).

Similarly, a sodium ion channel can exist in eight different states, and the corresponding kinetic scheme is given by Fig. 2 where $[m_i h_j]$ is the number of sodium ion channels

$$[n_0] \underset{\beta_n}{\overset{4\alpha_n}{\rightleftarrows}} [n_1] \underset{2\beta_n}{\overset{3\alpha_n}{\rightleftarrows}} [n_2] \underset{3\beta_n}{\overset{2\alpha_n}{\rightleftarrows}} [n_3] \underset{4\beta_n}{\overset{\alpha_n}{\rightleftarrows}} [n_4]$$

FIG. 1. Markov model for potassium ion channels.

with i open m gates and j open h gates. So $[m_3 h_1]$ is the number of open sodium ion channels (see Fig. 2).

At a specific time t, if the transition rate of ion channels from state 1 to state 2 is γ, then each ion channel in state 1 will transfer to state 2 in time interval δt with probability $\gamma \delta t$. We can randomly choose transition channel number δn_{12} from state 1 to state 2 in time interval δt from a binomial distribution,

$$P(\delta n_{12}) = \binom{n_1}{\delta n_{12}} p^{\delta n_{12}} (1-p)^{(n_1 - \delta n_{12})}, \tag{5}$$

where n_1 is the ion channel number in state 1 and p is $\gamma \delta t$. We use the forward Euler integration and choose the time interval δt to be 10 μs. In each time interval, we update the voltage-dependent transition rates, determine randomly the transition channel number between two nearby states, and update the ion channel distribution at each state and membrane potential.

C. Compartmental models

The main assumption of the compartmental model is that small pieces of a cable can be treated as isopotential elements, so that the continuous structure of a neuronal cable can be treated approximately as a set of linked discrete elements [24]. The compartmental model replaces the continuous differential equations of the analytical model by a set of ordinary differential equations. If the continuous cable system is divided into sufficiently small compartments, it is reasonable to assume that each compartment is isopotential and spatially uniform in properties.

A chain of three cylindrical dendritic compartments is shown in Fig. 3. The three compartments are sufficiently small to be considered isopotential. Assuming the membrane is passive, we can plot the equivalent circuit of the three compartments in Fig. 3. The mathematical expression of compartmental models of neurons is a set of ordinary differential equations. Each equation is derived from Kirchhoff's current law. In the jth compartment, the net current i_{m_j} through the membrane equals the longitudinal current that enters the compartment minus the longitudinal current that leaves the compartment. Then the membrane current through the jth compartment is

$$\begin{array}{ccccccc}
[m_0h_1] & \underset{\beta_m}{\overset{3\alpha_m}{\rightleftarrows}} & [m_1h_1] & \underset{2\beta_m}{\overset{2\alpha_m}{\rightleftarrows}} & [m_2h_1] & \underset{3\beta_m}{\overset{\alpha_m}{\rightleftarrows}} & [m_3h_1] \\
\alpha_h \uparrow \downarrow \beta_h & & \alpha_h \uparrow \downarrow \beta_h & & \alpha_h \uparrow \downarrow \beta_h & & \alpha_h \uparrow \downarrow \beta_h \\
[m_0h_0] & \underset{\beta_m}{\overset{3\alpha_m}{\rightleftarrows}} & [m_1h_0] & \underset{2\beta_m}{\overset{2\alpha_m}{\rightleftarrows}} & [m_2h_0] & \underset{3\beta_m}{\overset{\alpha_m}{\rightleftarrows}} & [m_3h_0]
\end{array}$$

FIG. 2. Markov model for sodium ion channels.

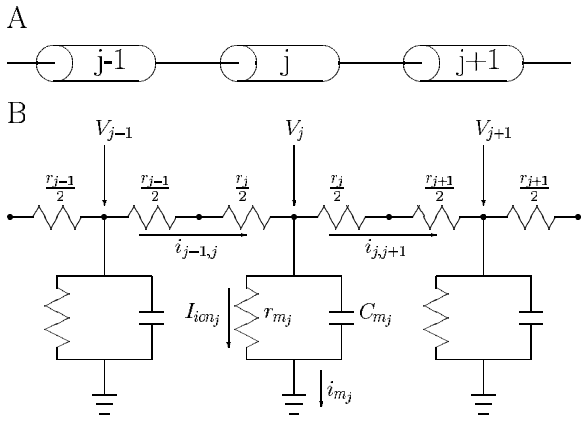

FIG. 3. (A) A chain of three cylindrical segments that are sufficiently short to be considered isopotential. (B) The equivalent circuit for the compartmental model of a chain of three successive small cylindrical segments of a passive dendritic membrane.

$$i_{m_j} = i_{j-1,j} - i_{j,j+1}, \tag{6}$$

where $i_{j-1,j}$ is the longitudinal current that flows from the $(j-1)$th to the jth compartments and $i_{j,j+1}$ is the longitudinal current that flows from the jth to the $(j+1)$th compartments.

The membrane current is the sum of the capacitative current and the net ionic current that flows through transmembrane. For the jth compartment, the membrane current can be expressed as

$$i_{m_j} = c_{m_j}\frac{dV_j}{dt} + I_{ion_j}, \tag{7}$$

where V_j is the membrane potential with respect to the resting potential. The longitudinal current can be expressed approximately as the voltage gradient between two nearby connected compartments divided by the axial resistance between the two compartments. Thus combining Eqs. (6) and (7), we can get the equation

$$c_{m_j}\frac{dV_j}{dt} + I_{ion_j} = \frac{V_{j-1} - V_j}{r_{j-1,j}} - \frac{V_j - V_{j+1}}{r_{j,j+1}} = (V_{j-1} - V_j)g_{j-1,j} - (V_j - V_{j+1})g_{j,j+1}, \tag{8}$$

where $r_{j-1,j}$ is the axial resistance between the $(j-1)$th and jth compartments and $g_{j-1,j}=1/r_{j-1,j}$ is the axial conductance between the $(j-1)$th and jth compartments. For the first compartment in a chain, only the second term for the longitudinal current appears on the right-hand side of the equations. For the last compartment in a chain, only the first term for the longitudinal current appears on the right-hand side of the equations. If the geometrical and electrical parameters of the axon are uniform, then $c_{m_j}=\pi d\Delta x C_m$, and $g_{j-1,j}=g_{j,j+1}=\frac{\pi d^2}{4\rho_a \Delta x}$, where d is the diameter of the axon, Δx is the length of each compartment, C_m is the specific membrane capacitance, and ρ_a is the specific axoplasmic resistivity. Putting the above formula into Eq. (8), we can get the equation

$$\frac{dV_j}{dt} = -\frac{1}{\pi d\Delta x C_m}I_{ion_j} + \frac{d}{4\rho_a C_m \Delta x^2}(V_{j-1} - 2V_j + V_{j+1}). \tag{9}$$

The term I_{ion_j} can embody properties of many types of channels in neural membranes. In this paper, there are the leakage current, the sodium ion channel current, and the potassium ion channel current in the ion channel cluster region. In this region, the term can be expressed as

$$I_{ion_j} = g_L(V - V_L) + g_{\mathrm{K}}(V - V_{\mathrm{K}}) + g_{\mathrm{Na}}(V - V_{\mathrm{Na}}). \tag{10}$$

So, in the ion channel cluster region, Eq. (9) can be rewritten as

$$\frac{dV_j}{dt} = -\frac{g_L(V_j - V_L) + g_{\mathrm{K}}(V_j - V_{\mathrm{K}}) + g_{\mathrm{Na}}(V_j - V_{\mathrm{Na}})}{\pi d\Delta x C_m} + \frac{d}{4\rho_a C_m \Delta x^2}(V_{j-1} - 2V_j + V_{j+1}). \tag{11}$$

In the unmyelinated cable region, the term I_{ion_j} only embodies the leakage current term, and the term can be simply expressed as

$$I_{ion_j} = g_L(V - V_L). \tag{12}$$

So, in the unmyelinated cable region, Eq. (9) can be rewritten as

$$\frac{dV_j}{dt} = -\frac{g_L(V_j - V_L)}{\pi d\Delta x C_m} + \frac{d}{4\rho_a C_m \Delta x^2}(V_{j-1} - 2V_j + V_{j+1}). \tag{13}$$

III. RESULT

We use the binomial method to compute results from the stochastic HH equations and analyze a spike train with 10 000 spikes. In order to verify the accuracy of our simulation, we have (i) verified that when the ion channel number is large, the simulation result of the stochastic HH equations approaches to that of the deterministic HH equations and (ii) verified that the results agree with those of [22]. We consider two ion channel clusters connected by an unmyelinated axon. The unmyelinated axon is divided into ten compartments. The parameters of the axonal system are given in Table I. The parameters related to the properties of the cable are adopted from [15], and the parameters related to the properties of ion channels are adopted from [23].

If there is no coupling between two ion channel clusters, the two clusters will generate spontaneous spiking independently. If we choose a very large distance between two ion channel clusters, they can be considered as two independent clusters. Figure 4 illustrates the spontaneous spiking of two approximately independent ion channel clusters. As shown in Fig. 4, the spontaneous spiking times of two approximately independent ion channel clusters are independent and not correlated. If we set the distance between two clusters to 20 μm, then the two ion channel clusters are coupled. Figure 5 illustrates the spontaneous spiking of two coupled ion

TABLE I. Axonal parameters. The parameters related to the properties of the cable are adopted from [15], and the parameters related to the properties of ion channels are adopted from [23].

Axon diameter (d)	2 μm
Membrane capacitance (C_m)	1 μF/cm^2
Axoplasmic resistivity (ρ_a)	80 Ω cm
Length of each compartment	2 μm
Na^+ density in the ion channel cluster (ρ_{Na})	60/μm^2
K^+ density in the ion channel cluster (ρ_K)	20/μm^2
Conductance of each ion channel (γ_{Na}, γ_K)	20 pS
Na^+ reversal potential (V_{Na})	50 mV
K^+ reversal potential (V_K)	−77 mV
Leakage reversal potential (V_L)	−54.4 mV
Leakage current conductance (g_L)	0.3 mS/cm^2
Transition rate (α_n)	$\alpha_n=\frac{0.01(V+55)}{1-e^{-(V+55)/10}}$
Transition rate (β_n)	$\beta_n=0.125e^{-(V+65)/80}$
Transition rate (α_m)	$\alpha_m=\frac{0.1(V+40)}{1-e^{-(V+40)/10}}$
Transition rate (β_m)	$\beta_m=4e^{-(V+65)/18}$
Transition rate (α_h)	$\alpha_h=0.07e^{-(V+65)/20}$
Transition rate (β_h)	$\beta_h=\frac{1}{1+e^{-(V+35)/10}}$

channel clusters. As shown in Fig. 5, the spontaneous spiking times of two coupled ion channel clusters are synchronized.

From Fig. 5, we find that the spiking times of two synchronized spikes are not exactly the same. The spiking time difference between two synchronized spikes is the action potential propagation time between the two ion channel clusters. The average spiking time difference between 200 pairs of synchronized spikes is 1.9 ms. The maximal time difference of the 200 pairs of spikes is 2.9 ms. If the spiking time difference between two spikes is less than 3 ms, we consider the two spikes to be synchronized. In order to measure the synchronization strength, we calculate the average consecutive synchronized spiking number (SSN), which is shown in Fig. 5. In our simulation, we first calculate 10 000 spikes for one cluster, then calculate the average consecutive synchronized spiking number.

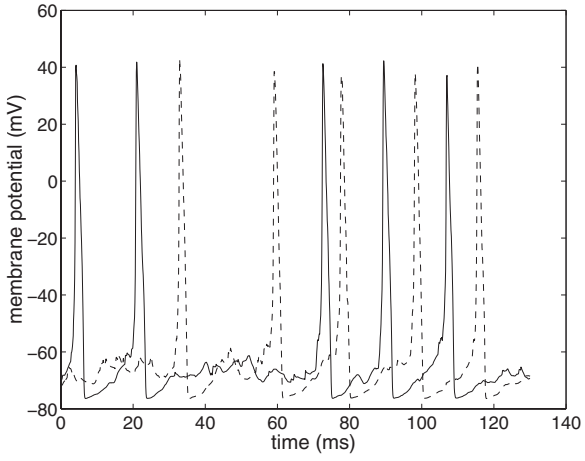

FIG. 4. The spontaneous spikes of two independent ion channel clusters.

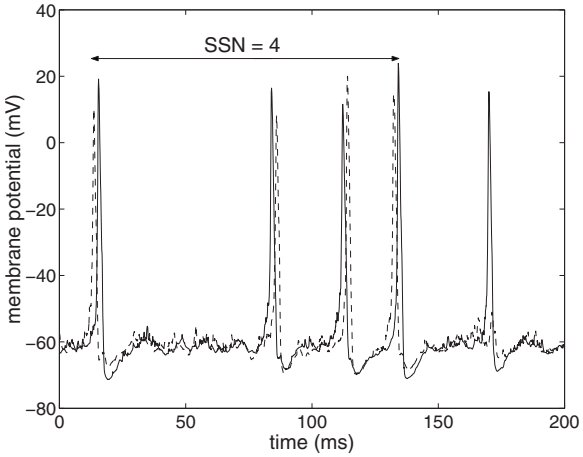

FIG. 5. The spontaneous spikes of two coupled ion channel clusters.

A. Effects of axonal parameters

We can consider the coefficient $\frac{d}{4\rho_a C_m \Delta x^2}$ of the second term on the right-hand side of Eq. (9) as the coupling strength. According to common scientific sense, the spiking synchronization will increase with increased coupling strength and vice versa. In order to measure the effect of the coupling strength on the spiking synchronization, we calculate the synchronized spiking number versus the coupling strength. First, we fix the axonal parameters as the values shown in Table I. Then we decrease the specific membrane capacitance (C_m), the specific electrical resistivity of the cytoplasmic core (ρ_a), and the axonal length (Δx) and increase the axon diameter (d) with the same rate: consequently, the coupling strength will increase. The effect of the coupling strength is shown in Fig. 6. As Fig. 6 shows, increasing the coupling strength increases the synchronized spiking number and vice versa. The effect is dramatic and approximately exponential.

In order to measure the effect of each individual axonal parameter, we consider the effects of the specific membrane capacitance, the specific electrical resistivity of the cytoplasmic core, the axon diameter, and the axonal length on the synchronized spiking number, respectively. When we con-

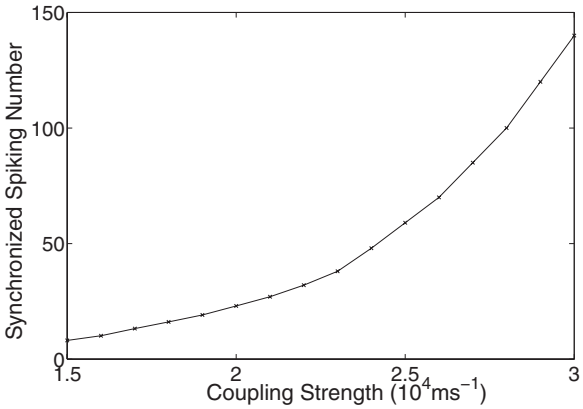

FIG. 6. The effect of the coupling strength.

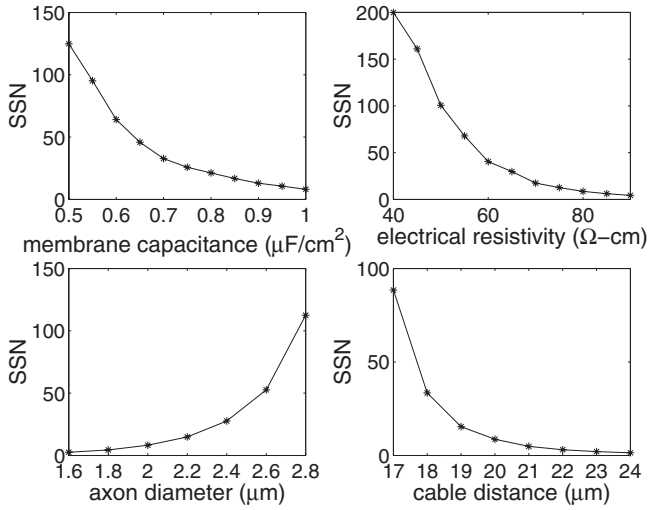

FIG. 7. The effects of axonal parameters on the synchronized spiking number. The effects of the specific membrane capacitance, the specific electrical resistivity of the cytoplasmic core, the axon diameter, and the cable length on the synchronized spiking number, respectively.

sider the effect of one parameter listed above, we fix the other parameters as the values shown in Table I. The effects of axonal parameters are shown in Fig. 7. As shown in Fig. 7, the synchronized spiking number will decrease if the specific membrane capacitance, the specific electrical resistivity, and the cable length are increased; if the axon diameter is increased, the synchronized spiking number will increase. The effect is dramatic and approximately exponential. It is clear that if ρ_a, C_m, and Δx are increased, the coupling strength will decrease. If d is increased, the coupling strength will increase. Increasing the coupling strength increases the synchronized spiking number and vice versa.

B. Effect of the cluster length distribution

Now we fix the total length of two ion channel clusters as 4 μm, fix the parameters as the values shown in Table I, and change the length of one cluster. The synchronized spiking number versus the length of the ion channel cluster is shown in Fig. 8. Because the system is symmetric about the middle point, where the length of each cluster is 2 μm, we first calculate the synchronized spiking number with the length of cluster 1 ranging from 0.6 to 3.4 μm, then calculate the average value about the middle point. As shown in Fig. 8, when two ion channel clusters have the same area, the synchronized spiking number is less than the maximal value, and the synchronization effect is most dramatic. It agrees with the real biological myelinated axon, where nodes are distributed homogeneously and each node has approximately the same area.

C. Effect of the cluster length

Now we fix the parameters as the values shown in Table I and change the length of each ion channel cluster simultaneously. The synchronized spiking number versus the length

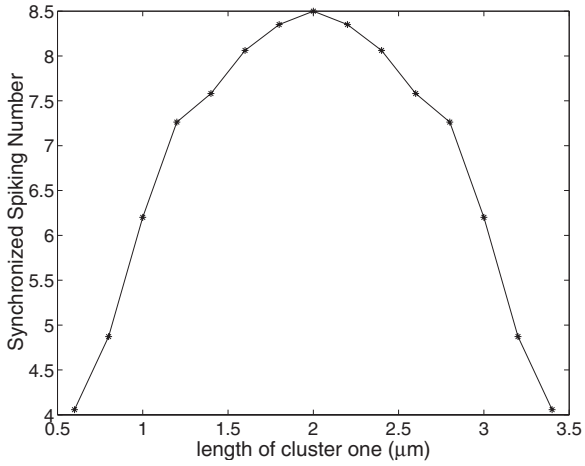

FIG. 8. The synchronized spiking number versus the length of ion channel cluster 1. The total length of two ion channel clusters is fixed as 4 μm.

of each ion channel cluster is shown in Fig. 9. As we increase the length of each ion channel cluster, the synchronized spiking number first increases: after reaching a maximal value, it then decreases. The spiking synchronization is due to charge propagation between two clusters. When there is a spike in cluster 1, then the charge will propagate from cluster 1 to cluster 2. If the quantity of the charge is large enough, the potential of cluster 2 will reach the threshold value, and a spike will be evoked. There is then a pair of synchronized spikes between the two clusters. If the quantity of the charge is not large enough, cluster 2 will not evoke a spike, and there will not be a pair of synchronized spikes between the two clusters. So whether the quantity of charge propagating between two clusters is above the threshold value is the main factor that determines the spiking synchronization of two clusters.

When the parameters of the axon are fixed, the quantity of the charge carried by one spike is approximately fixed. Then the threshold value of charge to evoke a spike is the main

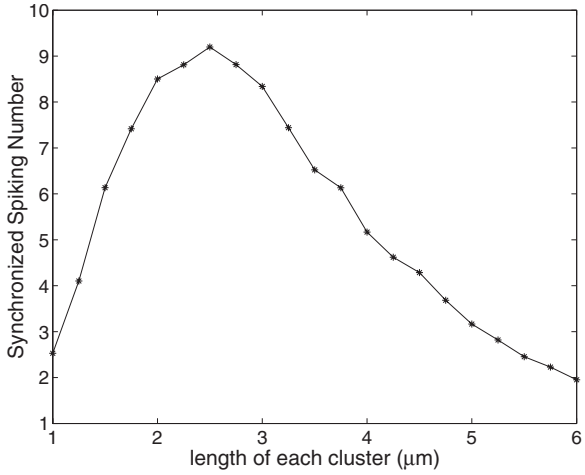

FIG. 9. The synchronized spiking number versus the length of each ion channel cluster. The length of each ion channel cluster changes simultaneously.

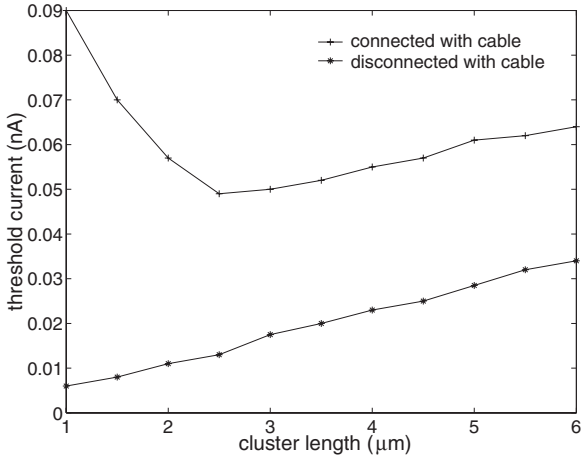

FIG. 10. The threshold values of the injected current for the ion channel cluster. The duration of the current pulse is fixed as 0.1 ms. In one case, the ion channel cluster is connected with an axon; in the other case, the ion channel cluster is isolated and is not connected with an axon.

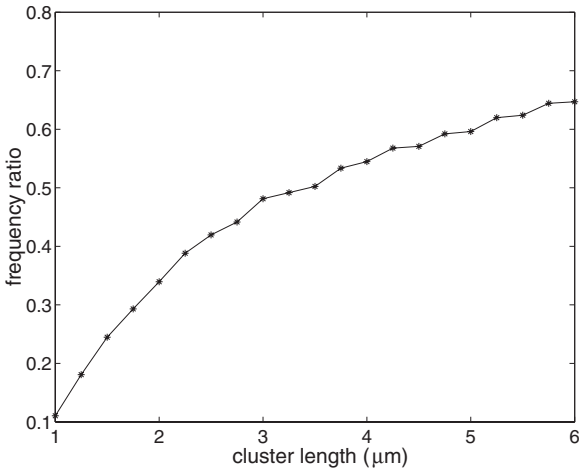

FIG. 11. The frequency ratio in two cases. In one case, the ion channel cluster is connected with the axon; in the other case, the ion channel cluster is isolated, and is not connected with the axon. The numerator is the spontaneous spiking frequency of case 1, and the denominator is the spontaneous spiking frequency of case 2.

factor to determine the spiking synchronization of two clusters. At first glance, one would expect that the smaller the area of the cluster, the smaller the threshold value of charge to evoke a spike is. Then the smaller the area of the cluster, the larger the synchronized spiking number is. But the simulation results in Fig. 9 show the opposite picture. The synchronized spiking number first increases with increasing cluster size. After reaching the maximal value, SSN decreases with increasing cluster size. We inject a current pulse in the ion channel cluster to calculate the threshold value to evoke a spike. The duration of the current pulse is fixed as 0.1 ms. We calculate the threshold value of the injected current in two cases. In one case, the ion channel cluster is connected with an axon; in the other case, the ion channel cluster is isolated and is not connected with an axon. The threshold values of the injected current in two cases are plotted in Fig. 10.

As Fig. 10 shows, in the case where the ion channel cluster is isolated, the threshold value of the injected current increases linearly with the cluster size. It is reasonable that the larger the area of the ion channel cluster is, more charge is needed to evoke a spike. In the other case where the ion channel cluster is connected with an axon, the threshold value of the injected current first decreases as the cluster size is increased, and after reaching the minimal value, it then increases with increasing cluster size. This phenomenon can explain why the synchronized spiking number first increases, reaches the maximal value, and then decreases.

When the action potential propagates from one ion channel cluster to the second ion channel cluster, charge moves in two directions in two different periods. During the first period, the voltage of the connected axon is higher than that of the second ion channel cluster. Charge moves from the connected axon to the second ion channel cluster, and the voltage of the second ion channel cluster will increase. When the voltage of the second ion channel cluster is higher than that of the connected axon, the second period is entered. In the second period, charge moves from the second ion channel cluster to the connected axon and will affect the voltage increase of the second ion channel cluster. The dissipation of charge by the connected axon will decrease the spiking of the second ion channel cluster. In order to measure the effect of charge dissipation from the channel cluster to the axon on the spiking of the ion channel cluster, we calculate the spontaneous spiking frequencies in two cases. In one case, the ion channel cluster is connected with the axon; in the other case, the ion channel cluster is isolated and is not connected with the axon. We calculate the ratio of spontaneous spiking frequencies in the two cases versus the length of ion channel cluster and plot it in Fig. 11.

As shown in Fig. 11, the ratio of spontaneous spiking frequencies increases with the length of the ion channel cluster. When the length of the ion channel cluster is small, the ratio is as small as 10%; when the length of the ion channel cluster is large, the ratio reaches 60%. When the size of the ion channel cluster is small, the effect of charge dissipation by the axon is dramatic, and the firing threshold is large. When the size of the ion channel cluster is increased, the ratio of the spontaneous spiking frequency increases. This mechanism will cause the threshold value of the ion channel cluster connected with the axon to decrease. On the other hand, the threshold value of the isolated ion channel cluster will increase due to increasing membrane area. This mechanism will cause the threshold value of the ion channel cluster connected with the axon to increase. There is a competition between the two mechanisms. When the length of the ion channel cluster is approximately 2.5 μm, the competition induces the optimal value. The threshold value of the injected current reaches the minimum when the synchronized spiking number has a maximum.

IV. DISCUSSION AND CONCLUSION

We considered the spiking synchronization of two coupled ion channel clusters. We used the synchronized spik-

ing number to describe synchronization strength. The axonal parameters, such as the specific membrane capacitance, the specific electrical resistivity, and the axon diameter, affect the synchronized spiking number exponentially. The coefficient $\frac{d}{\rho_a C_m}$ is used to describe the coupling strength [25]. Increasing the axon diameter (d) and decreasing the specific membrane capacitance (C_m) and the specific electrical resistivity (ρ_a) will increase the synchronized spiking number dramatically. It is known that the velocity of spike propagation will be proportional to the axon diameter [26]. On the other hand, increasing the axon diameter will also be beneficial for the spiking synchronization. In myelinated axons, myelines isolate the membrane and decrease the membrane capacitance. Decreasing the membrane capacitance can decrease the time constant of the axon and increase the spike propagation speed [23]. On the other hand, it is also shown in the paper that decreasing the membrane capacitance can increase the spiking synchronization.

It is shown that two ion channel clusters exhibit maximal spiking synchronization when they have the same size. Correspondingly, in biological systems the length of the nodes of Ranvier in myelinated axon is uniform. It is also shown that there is an optimal size of ion channel clusters with maximal spiking synchronization. The length of ion channel clusters with the maximal synchronized spiking number is approximately 2.5 μm. This value accords with the length of the nodes of Ranvier in the myelinated axon [27]. In order to explain the optimal phenomenon of the synchronized spiking number, we calculate the threshold value of the injected current of the ion channel cluster connected with the axon. Correspondingly, the threshold value of the injected current has a minimal value when the length of the ion channel cluster is approximately 2.5 μm. There are two mechanisms that affect the threshold value of the injected current. First, when increasing the size of the ion channel cluster, the threshold value of the injected current of an isolated ion channel cluster will increase. Second, when increasing the area of the ion channel cluster, the effect of charge dissipation by the axon will decrease and cause the threshold decrease relatively. The competition of the two mechanisms generates an optimal threshold value of the injected current and produces an optimal ion channel cluster length with the maximal spiking synchronization.

[1] M. G. Rosenblum, A. Pikovsky, C. Schafer, P. A. Tass, and J. Kurths, *Neuro-Informatics and Neural Modelling* (North-Holland, Amsterdam, 2001).

[2] C. Hayashi, *Nonlinear Oscillations in Physical Systems* (McGraw-Hill, New York, 1964).

[3] P. Landa, *Nonlinear Oscillations and Waves in Dynamical Systems* (Kluwer Academic, Dordrecht, 1996).

[4] M. G. Rosenblum, A. S. Pikovsky, and J. Kurths, Phys. Rev. Lett. **76**, 1804 (1996).

[5] D. Bramble and D. Carrier, Science **219**, 251 (1983).

[6] L. Glass and M. C. Mackey, *From Clocks to Chaos: The Rhythms of life* (Princeton University Press, Princeton, NJ, 1988).

[7] J. Sturis, C. Knudsen, N. M. O'Meara, J. S. Thomsen, E. Mosekilde, E. Van Cauter, and K. S. Polonsky, Chaos, **5**, 193 (1995).

[8] A. Neiman, X. Pei, D. Russell, W. Wojtenek, L. Wilkens, F. Moss, H. A. Braun, M. T. Huber, and K. Voigt, Phys. Rev. Lett. **82**, 660 (1999).

[9] J. R. Clay and A. M. Kuzirian, J. Neurobiol. **45**, 172 (2000).

[10] J. R. Clay and A. M. Kuzirian, Biophys. J. **76**, A223 (1999).

[11] C. Hilderbrand and S. G. Waxman, Brain Res. **258**, 23 (1983).

[12] R. W. Turner *et al.*, J. Neurosci. **14**, 6453 (1994).

[13] C. C. Chow and J. A. White, Biophys. J. **71**, 3013 (1996).

[14] R. F. Fox, Biophys. J. **72**, 2068 (1997).

[15] A. L. Hodgkin and A. F. Huxley, J. Physiol. (London) **117**, 500 (1952).

[16] A. Fulinski, Z. Grzywna, I. Mellor, Z. Siwy, and P. N. R. Usherwood, Phys. Rev. E **58**, 919 (1998).

[17] Z. Siwy and A. Fulinski, Phys. Rev. Lett. **89**, 158101 (2002).

[18] S. Mercik, K. Weron, and Z. Siwy, Phys. Rev. E **60**, 7343 (1999).

[19] S. B. Lowen, L. S. Liebovitch, and J. A. White, Phys. Rev. E **59**, 5970 (1999).

[20] B. Hille, *Ionic Channels of Excitable Membranes*, 2nd ed. (Sinauer Associate, Sunderland, MA, 1992).

[21] B. Sakmann and E. Neher, *Single-Channel Recording*, 2nd ed. (Plenum, New York, 1995).

[22] E. Schneidman, B. Freedman, and I. Segev, Neural Comput. **10**, 1679 (1998).

[23] C. Koch, *Biophysics of Computation: Information Processing in Single Neurons* (Oxford University Press, New York, 1999).

[24] I. Segev and R. E. Burke, *Methods in Neuronal Modeling: From Ions to Networks* (MIT Press, Cambridge, MA, 1998).

[25] R. Nossal and H. Lecar, *Molecular and Cell Biophysics* (Addison-Wesley, Redwood City, CA).

[26] J. M. Ritchie, Proc. R. Soc. London, Ser. B **217**, 29 (1982).

[27] R. B. Rogart and J. M. Ritchie, *Physiological Basis of Conduction in Myelinated Nerve Fibers* (Plenum Press, New York, 1977).